INTEGRATED EXPLORATORY STUDY OF ANOMALIES DUE TO HYDROCARBON IN WESTERN FALCÓN BASIN, VENEZUELA

R. De La Rosa[1]*, S. Yépez[1], M. Aldana[1], V. Costanzo-Alvarez[1], R. Saavedra[2] y A. Martin[2].

[1] Simón Bolívar University, Caracas Venezuela.
[2] Fundación Instituto de Ingeniería, Caracas Venezuela.
* e--mail: robertoadlr@gmail.com

ABSTRACT

A spectral analysis of an ASTER image was performed in an oil prospective area of The Cerro Pelado Anticlinal (CPA) in the Western Falcón Basin, Venezuela, to determine the existence of mineral alteration zones, related to the presence of hydrocarbon seepages, in order to guide the oil exploration to better defined areas, integrating a fieldwork, Magnetic Susceptibility (MS) and S-ratio measurements, Isothermal Remagnetization Curves (IRM), (decomposed by applying a Direct Spectral Analysis (DSA)), laboratory spectroradiometry, X-ray Diffraction (XRD) and Geochemical analysis. The analysis was done over 127 samples of rock and soil (59 from the surface, 47 taken at 0.5 m depth and 21 from 1 m depth). The results indicate the presence of three areas of mineral alteration, identified through the processing of a satellite image by anomalies of Kaolinite, FE3+, Dolomite, Clay and associated with the presence of hydrocarbons. Alteration areas are characterized by low MS values, between 0-4 χ [SI] and a range of 0.4 to 0.7 on behalf of the S-ratio. The DSA analysis indicated a large presence of goethite and hematite. Although low levels of MS were measured, magnetite was also observed in some samples.

Keywords: ASTER, S-ratio, MS, IRM, DSA, DRX, Hydrocarbons.

RESUMEN

Con el objetivo principal de determinar la existencia de zonas de alteración mineral relacionadas con la presencia de infiltraciones de hidrocarburo, se realizó el análisis espectral de una imagen ASTER en un área prospectiva del Anticlinal de Cerro Pelado (ACP), en la Cuenca Occidental de Falcón, Venezuela. Se intenta orientar la exploración petrolera a zonas mejor delimitadas, integrando mediciones de campo, Susceptibilidad Magnética (MS), Cociente-S, Curvas de Remanencia Magnética Isotermal (IRM) (descompuestas aplicando un Análisis Espectral Directo (DSA)), Espectroradiometría de laboratorio, Difracción de rayos-X (DRX) y Geoquímica. El análisis se hizo sobre 127 muestras de suelo y roca (59 en superficie, 47 a 0.5 m y 21 a 1 m de profundidad). Los resultados indican la presencia de tres áreas de alteración mineral, identificadas a través del procesamiento de la imagen satelital, correspondientes a anomalías de Caolinita, FE3+, Dolomita, Arcilla y asociadas a la presencia de hidrocarburos. Las áreas de alteración se caracterizan por bajos valores de MS, entre 0-4 χ [SI] y valores de cociente-S entre 0.4 a 0.7. Los análisis de DSA indican la presencia mayoritaria de goethita y hematita. A pesar de los bajos valores de MS medidos, se observó magnetita en algunas muestras.

Palabras Clave: ASTER, Cociente-S, MS, IRM, DSA, DRX, Hidrocarburos

Introduction

It is known that all reservoirs exhibit some kind of leakage, at least until subsurface levels, which is known as micro seeps. In both cases, visible or not, the presence of hydrocarbons generates a series of anomalies due to chemical, physical and mineralogical alterations, produced by the hydrocarbons in contact with its surroundings, generating observable and measurable evidence in surface (Schumacher, 1996; Donovan, *et al.*, 1979;. Foote, 1992, 1996; Saunders, *et al.*, 1991). The present research is based on the fact that surface alterations are generated by the vertical migration of hydrocarbons from underlying reservoirs, inducing distinct spectral characteristics to those observed in laterally equivalent rocks, which satellite remote sensing are able to detect through various techniques of digital image processing. (Yang, *et al*., 1999; Khan and Jacobson, 2008; Petrovic, *et al.*, 2008; Kruse, *et al.*, 2011 and Salati, *et al.*, 2014). Similarly, MS, S-ratio and IRM curves measurements have been employed before in soil and rock samples *e.g.,* (Aldana, *et al*., 1999, 2003, 2011; Constanzo-Alvarez, *et al.*, 2000, 2006.; Diaz, *et al*., 2000; Guzman, *et al*., 2010 and Da Silva, *et al*., 2010), as a possible alternative to detect anomalous magnetization and its relationship with the presence of hydrocarbons

Combining the methods indicated above, we attempt to locate and characterize efficiently and with low economical cost these changes and their relationship to the presence of hydrocarbons, to orient oil exploration in the CPA prospective area at the Western Falcón Basin, Venezuela, trying to increase the degree of certainty. To achieve this, we integrate the digital processing of an ASTER image, MS measurements, S-ratio, IRM curves, the decomposition of these curves were obtained by applying DSA, laboratory spectrometry, XRD, and geochemistry; conducted on 127 soil and rock samples collected on a fieldwork, with the following distribution: 59 at Surface, 47 at 0.5 m and 21 at 1 m depth, all from The Cerro Pelado Formation (CPF).

Methodology and results

An ASTER image was used, covering an area of 1800 Km², with a level of processing L1A, which has three subsystems: the visible and near infrared (VNIR), the shortwave infrared (SWIR) and thermal infrared (TIR), with a total of 14 bands. The pre-processing of the ASTER image was made through the radiometric and geometric calibration, upgrading the image to a L1B processing level. The atmospheric correction was performed to obtain the reflectance image. Once this image was obtained, we proceeded with the multispectral processing of the ASTER image, which applies the method of bands ratio oriented to identify $FE3^{+}$, dolomite, kaolinite and clay. The method of main components (conventional, oriented and Crosta applied to kaolinite) was also used. Then a hyper spectral processing on the reflectance image was applied, using the transformation fraction of noise, pixel purity rate and a spectral analysis through an n-dimensional display, to finally classify through the spectral angle method and the matches tuned mix filter method (Kruse, *et al*., 2011; Van Der Meer and De Jong, 2006). The results obtained after the digital processing of an ASTER image, allowed reducing the exploration area to about 35 Km², in accordance with the observed anomalies. This area is characterized by its scarce vegetation, specifically on the CPF at the CPA, in three areas, which have mineral alterations; they are also aligned with the prospective structure of the CPA and the presence of hydrocarbon seepages. This suggests that these alterations could be due to the presence of hydrocarbons. The three areas are characterized by high values of $Fe3^{+}$, clay, kaolinite and a decrease in the values of dolomite, compared with the mean response of the CPF; these results are consistent with those obtained by Salati, *et al*. (2014) and the alteration model introduced by Schumacher, (1996).

By having a better defined area, a fieldwork was conducted, with the main aim of collecting 127 samples of soil and rock, using hand tools for removal; 59 were collected at Surface, 47 at 0.5 m and 21 at 1 m depth, all over the CPF, inside and outside of the alteration areas (A, B and C), as shown in Figure 1. It is remarkable that, during the fieldwork, there were observed significant concentrations of sulfur and gypsum precipitations in surface, at areas close to the hydrocarbons seeps.

Ten spectral signatures were taken for each sample and then an average was carried out, generating a spectral library for 127 samples. We employ a laboratory spectroradiometer ASD Inc., which has a spectral range of 350-2500 [nm], a precision in wavelength of ± 1 [nm], a sampling interval of 1.4 [nm] between 350 to 1000 [nm] and 2 [nm] between 1000 and 2500 [nm] with light and temperature conditions controlled in the laboratory. An absorption peak around 2200 [nm] was shown by the laboratory spectral signatures in the samples that are within the alteration areas. This peak increases when the hydrocarbon seeps are approached and it is associated with kaolinite, according to comparisons made against the USGS spectral library (Clark, *et al*., 2007).

Geochemical analysis were performed on 20 samples (10 inside of the alteration halos and 10 outside); particularly XRD and clays separations were used, following the methodology applied by Petrovic, *et al*., (2012). An arithmetic mean was used as pattern of comparison between both populations. The correlation histogram for the kaolinite over other clays indicates that the samples belonging to the alteration halos have, on average, 5.8% more clay. When the clays separation was performed, it was observed that, on average, 83% of the clay was kaolinite for the samples within the halo. In external samples, this switches to only 60%. The XRD of the samples near to the hydrocarbon seeps, could directly detect kaolinite, natrajarosita, jarosite, illite and chlorite, all of them indicators of mineralogical alterations due to the presence of hydrocarbons (Van Der Meer, De Jong, 2006). MS measures were performed on 127 samples with a Bartington Susceptometer at room temperature. S-ratio (IRM -0.3T / IRM + 2T) measurements were also performed using an ASC Scientific pulse magnetizer model IM-10-3. The magnetization was measured through a spinning magnetometer MolspinLimited. Three maps were generated, for the analysis of the MS and S-ratio results, one for surface samples, another for samples around 0.5 m and one for samples at 1 m depth, trying to better observe the spatial distribution of the results.

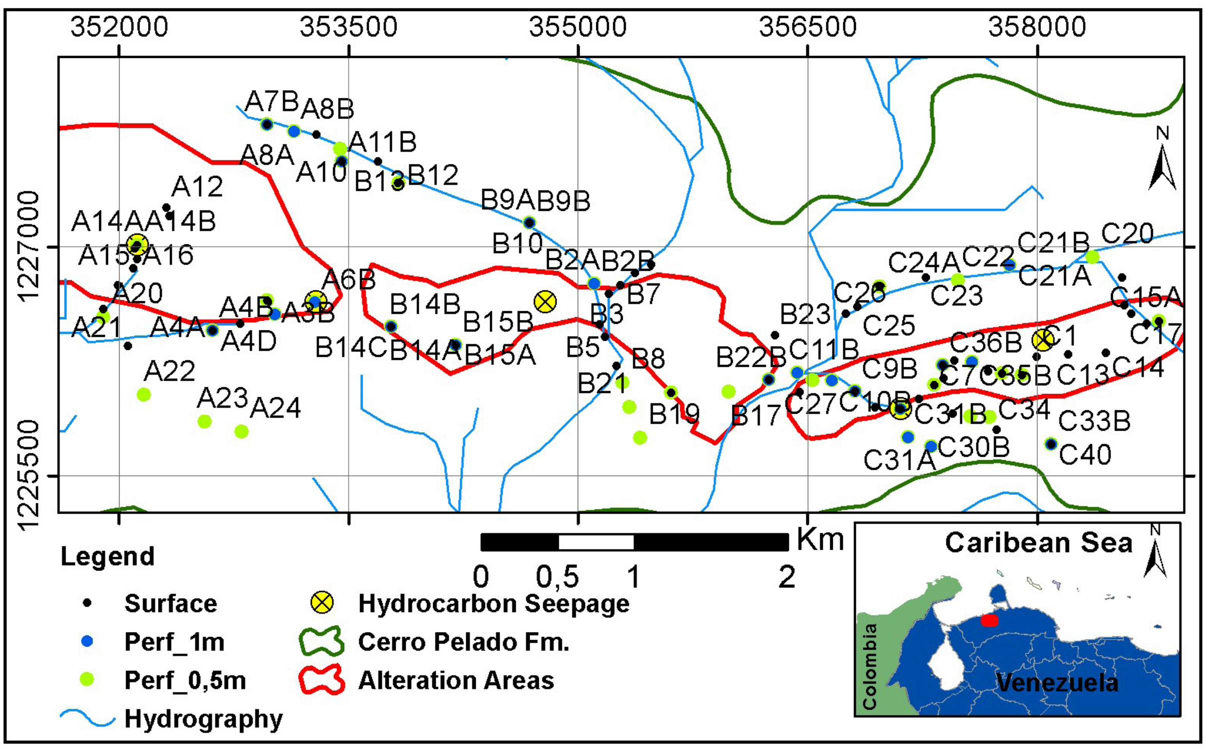

Figure 1. Location of the study area and collected samples. The Longitude and Latitude are in UTM WGS84 Z19N

MS results were not conclusive, because, in general, all samples have low susceptibility values, between 0 and 4 χ [SI], resulting in a homogeneous distribution throughout the three alteration halos. Also it was observed that the range of MS values increased with depth, which shows the effects of weathering on the samples *in situ*. In the S- ratio maps (see Figure 2), values between 0.55 and 0.75 are observed, within the alteration halos near the hydrocarbon seepages. The low MS values and medium S-ratios obtained suggest that the mineral alterations are not characterized by the presence of authigenic magnetite as the main magnetic mineral. Furthermore, it is clear the alignment of the hydrography, calculated from the digital elevation model derived from the ASTER image (with 30 m of spatial resolution), with the low values of S-ratio, mainly in surface samples maps and the 0.5 m depth maps, suggesting that the effects of erosion are minimal at 1m depth.

14 profiles were extracted from the maps, over the samples acquired in the field, integrating the results of bands ratios associated with kaolinite, dolomite, $FE3^{+}$ and clay from the multispectral satellite image processing, considering in addition, the topography, the S-ratio and the MS measurements. In Figure 3a, it can be observed the profile 2 location, traced on the samples derived from the drilling of approximately 1m deep, arranged from west to east. In Figure 3b, the closest points to the hydrocarbons seeps are marked by the red vertical lines. It can be clearly observed the increase of $FE3^{+}$, clay and kaolinite values, while the values of dolomite decrease. The MS, generally, has a uniform behaviour (low values), the S-ratio is represented by high values; also a lack of dependence with the topography can be observed at this depth

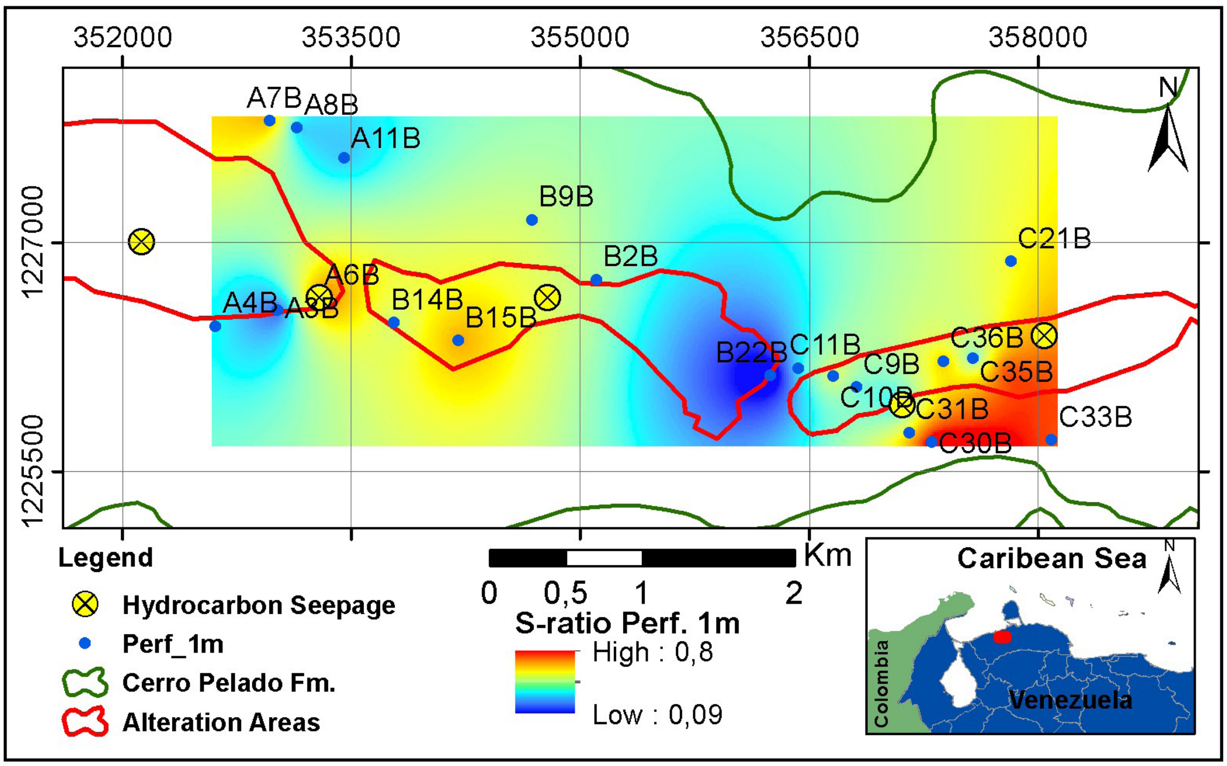

Figure 2. S-ratio map for samples at 1m depth. The Longitude and Latitude are in UTM WGS84 Z19N

Finally, 7 samples (A14a, A6B, B15B, B5, C13, C32B, and C35A) were selected, distributed in three alteration halos, and their IRM curves obtained. These curves were analyzed with the DSA method (Aldana, *et al.,* 2011), trying to identify the main magnetic minerals and their relative concentration at the alterations areas (see Figure 4). In the samples A6B, B5 and C35A, each belonging to each alteration halo (A, B and C respectively), the analysis indicates, in average, a mixture of goethite (38%) and hematite (62%); also the presence of magnetite is observed in the B15, C13 and C32B samples in different relative concentrations.

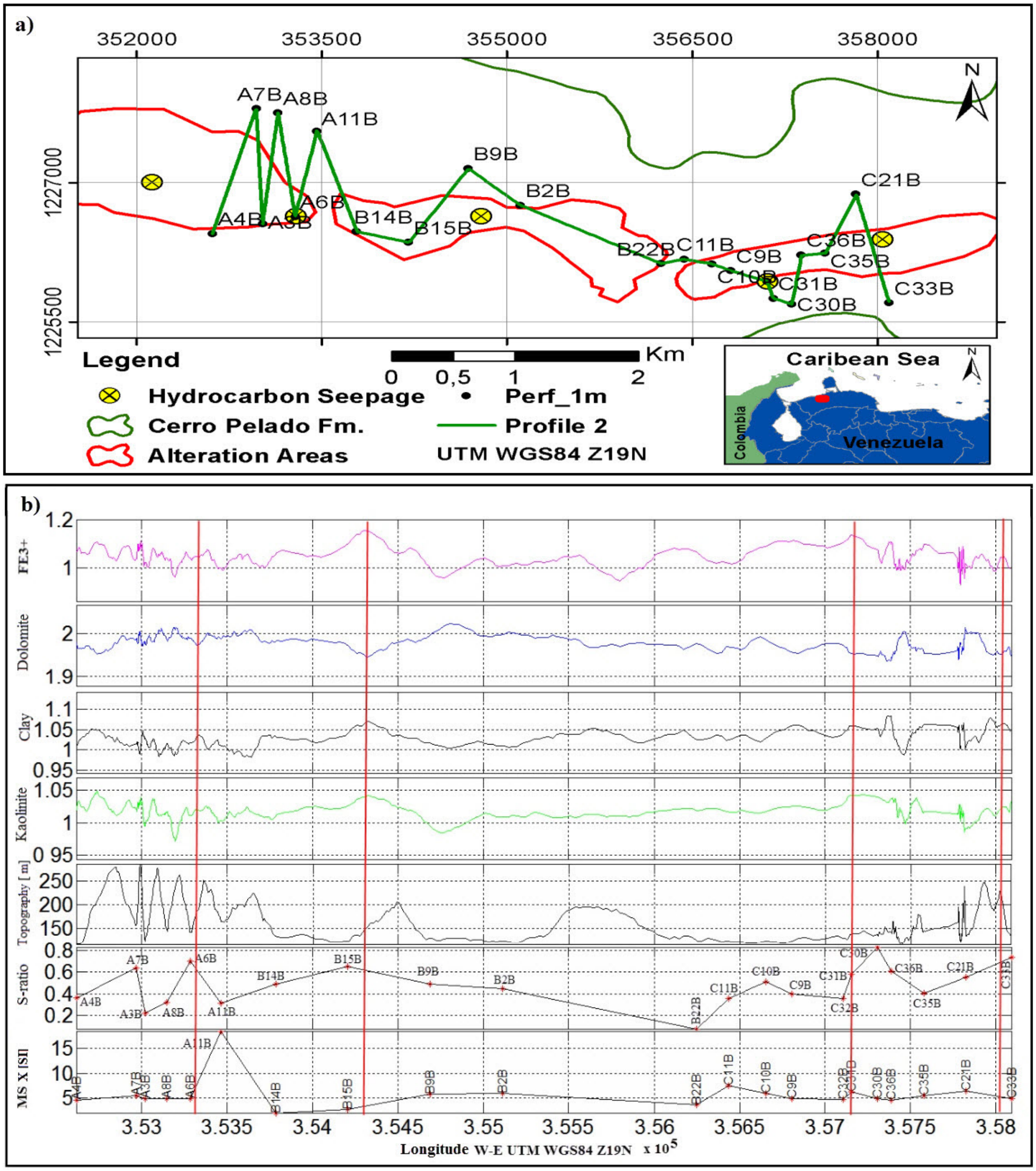

Figure 3. a) Location of Profile 2 on the samples at 1m depth, sorted by Longitude W-E. b) Results for the Profile 2. Noting values FE3^{+}, Dolomite, Clay, kaolinite, topography, S-ratio and Magnetic Susceptibility

Conclusions

The integration of the applied methodologies indicates the existence of, at least, three alteration areas, probably due to the presence of hydrocarbons, in the prospective area of the CPA at the CPF of the Western Falcón Basin, Venezuela. These alteration areas show a spatial alignment with the structure and the hydrocarbon seepages observed *in situ*. The digital ASTER image processing, regardless of the low

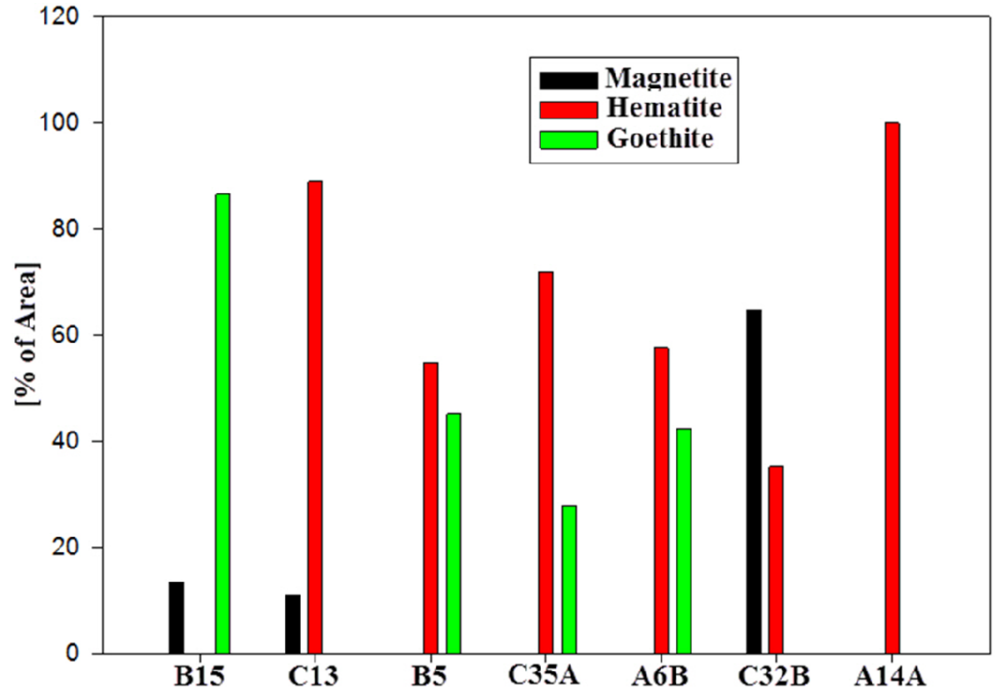

Figure 4. Results of the direct signal analysis (DSA) on 7 samples belonging to the alteration halos

spatial resolution of the bands used (30m), detected and characterized the mineralogical anomalies due to the increase of the relative concentrations of kaolinite, clay and $FE3^{+}$; however, the dolomite decreases. All these characteristic features of alterations associated with hydrocarbons were confirmed by the laboratory spectroscopy, XRD and geochemical analysis. Through this integration it was possible to quantify the increase of the relative concentrations of kaolinite and other minerals as natrajarosita, jarosite, chlorite and illite in the samples within alteration halos, obtaining on average, a 5.8% more clays. For these altered samples an 83% of the clay are conformed by kaolinite. However, for samples outside of the alteration areas, the kaolinite represents only 60% of the total clay.

The magnetic characterization of the alteration areas indicates low values of the susceptibility and average values of S-ratio, which suggest, that the alterations are associated, principally, to magnetic minerals other than the magnetite. The DSA analysis of the IRM curves indicates a combination of different relative concentrations of goethite and hematite associated with these alteration zones and probably due to the presence of hydrocarbons. In some samples it is observed the presence of magnetite in lesser proportion. These results may help to guide future oil exploration in the region, focusing resources in the alteration areas found, defined and characterized in the oil prospective zone of CPA.

References

Aldana M., Costanzo-Álvarez V., Vitiello D., Comenares L., Gómez G., 1999. Framboidal magnetic minerals and their possible association to hydrocarbons: La Victoria oil field (SW,Venezuela). *Geofís. Int., 38,* 137−152.

Aldana M., Costanzo-Álvarez V., Díaz M., 2003. Magnetic and mineralogical studies to characterize oil reservoirs in Venezuela. *The Leading Edge, 22,* 526−528.

Aldana, M., Costanzo-Álvarez, V., Gómez, L., González, C., Díaz, M., Silva, P., Rada, M., 2011. Identification of magnetic minerals related to hydrocarbon authigenesis in venezuelan oil fields using an alternative decomposition of isothermal remanence curves. *Stud. Geophys. Geod., 55,* 343-358.

Clark, R., Swayze, G., Wise, R., Livo, E., Hoefen, T., Kokaly, R., Sutley, S., 2007. USGS digital spectral library splib06a. *U.S. Geological Survey, Digital Data Series 231,* Available in *http://speclab.cr.usgs.gov/spectral.lib06.*

Costanzo-Álvarez V., Aldana M., Aristiguieta O., Marcano M., Aconcha E., 2000. Study of magnetic contrast in the Guafita Oil Field (southwestern Venezuela). *Phys. Chem. Earth, 25,* 437−445.

Costanzo-Álvarez V., Aldana M., Díaz M., Bayona G., Ayala C., 2006. Hydrocarbon-induced magnetic contrasts in some Venezuelan and Colombian oil wells. *Earth Planets Space, 58,* 1401−1410.

Da Silva, A., Costanzo-Álvarez, V., Hurtado, N., Aldana, M., Bayona, G., Guzmán, O., López-Rodríguez, D., 2010. Possible correlation between Miocene global climatic changes and magnetic proxies, using neuro fuzzy logic analysis in a stratigraphic well at the llanos foreland basin, Colombia. *Stud. Geophys. Geod., 54,* 607-631.

Díaz M., Aldana M., Costanzo-Álvarez V., Silva P., Perez A., 2000. EPR and magnetic susceptibility studies in well samples from some Venezuelan oil fields. *Phys. Chem. Earth A, 25,* 447−453.

Donovan T. J., Forgey R., Roberts A., 1979. Aeromagnetic detection of diagenetic magnetite over oil fields. *AAPG Bull., 63,* 245−248.

Foote R. S., 1992. Use of magnetic field aids in oil search. *Oil & Gas Journal, 4,* 137-141.

Foote R. S., 1996. Relationship of near-surface magnetic anomalies to oil-and gas-producing area, *Hydrocarbon Migration and Its Near-Surface Expression. AAPG Memoir, 66,* 111−126.

Guzmán, O., Costanzo-Álvarez, V., Aldana, M., Díaz, M., 2010. Study of magnetic contrasts applied to hydrocarbon exploration in the Maturín sub-basin (Eastern Venezuela). *LatinMag Special Issue #4, Stud. Geophys. Geod., 54. And Stud. Geophys. Geod., 55,* 359-376.

Khan, S. y Jacobson, S., 2008, Remote sensing and geochemistry for detecting hydrocarbon microseepages. *Geological Society of America Bulletin, 120(1/2),* 95-105.

Kruse, F., Taranik, J., Coolbaugh, M., Michaels, J., Littlefield, E., Calvin, W., Martini, B., 2011. Effect of Reduced Spatial Resolution on Mineral Mapping Using Imaging Spectrometry—Examples Using Hyperspectral Infrared Imager (HyspIRI)-Simulated Data. *Remote Sens., 3, 1584-1602.* Available*: www.mdpi.com/journal/remotesensing*

Petrovic, A., Khan, S. D., Chafetz, H., 2008. Remote detection and geochemical studies for finding hydrocarbon- induced alterations in Lisbon Valley, Utah. *Journal of Marine and Petroleum Geology, 25,* 696-705.

Petrovic, A., Khan, S. D., Thurmond, A. K., 2012. Integrated hyperspectral remote sensing, geochemical and isotopic studies for understanding hydrocarbon-induced rock alterations. *Mar. Pet. Geol., 35,* 292-308.

Salati, S., Van der Meer, F., van Ruitenbeeek, F., Naimi, B., 2014. Detection of alteration induced by onshore gas sepes from ASTER and WorldView-2 data. *Remote Sens., 6,* 3188-3209. Available*: www.mdpi.com/journal/remotesensing*

Saunders D., Burson K., Thompson C., 1991. Observed relation of soil magnetic susceptibility and soil gas hydrocarbon analyses to subsurface hydrocarbon accumulations. *AAPG Bull., 55,* 344−353.

Schumacher. D, 1996. Hydrocarbon – induced alteration of soils and sediments. *Hydrocarbon migration and its near – surface expression: AAPG Memoir 66,* 71-89.

Van Der Meer, F., De Jong, S., 2006. Imagin Spectrometry, Basic principles and prospective applications. *Published by Springer, Dordrecht, The Netherlands. 17-108.*

Yang, H., Zhang, J., van der Meer, F., Kroonenberg, S. B., 1999. Geochemistry and field spectrometry for detecting hydrocarbon microseepage. *Terra Nova, 10,* 231-235.